29th Congress of the International Council
of the Aeronautical Sciences
St. Petersburg, Russia; September 7–12, 2014

L1 ADAPTIVE ATTITUDE CONTROLLER FOR A TAIL-SITTER MAV IN HOVER FLIGHT

Wang Jin , Song Bifeng , Wang Liguang
School of Aeronautics , Northwestern Polytechnical University

Abstract

Since there exist several practical problems, hover flight control of tail-sitter vertical take-off and landing (VTOL) micro aerial vehicle (MAV) remains a challenging task all the time. This paper proposes a solution to this task, which combines the backstepping control architecture with L1 adaptive control theory. Aerodynamic moments of the wing are included thus the adaptation law is ensured to concentrate on the environmental disturbance. The output dynamic inversion is applied to determine the control surfaces deflection from control moments. These characters enable the controller to be transplanted to other VTOL MAV without retuning. The hover flight tests were conducted on a flying wing tail-sitter MAV, the results showed satisfactory tracking performance and disturbance resistance.

1 Introduction

Autonomously hovering and operating in a constrained environment, which enables a vertical take-off and landing(VTOL) Unmanned Aerial Systems(UASs) to perform stare surveillance or inside building search, will greatly expand the application field of UASs. Amid all the VTOL configurations, tail-sitter design possesses mechanical simplicity that conforms to the design philosophy of MUAVs and Micro aerial vehicles(MAVs). In consequence of this prospect, increasing interests are spurred in hovering control of tail-sitter miniature unmanned aerial vehicles(MUAVs) [1, 2]. Even so, hover control of indoor tail-sitter MAV is revealed to be a more challenging task compared with MUAVs in four aspects: larger states measurement noise, weak control effectiveness, disturbance sensitivity and modelling error due to tightened interaction between propeller slip stream and wing aerodynamics.

Aforementioned difficulties imply the L1 adaptive control theory as a feasible solution for indoor tail-sitter MAV hover control. The L1 adaptive controller utilizes low-pass filtered adaptive control signal, which theoretically balances system robustness and adaptation speed [3]. To deal with hover dynamics, which is a cascade nonlinear system, Mallikarjunan et al [4] developed three versions of L1 backstepping attitude controller. Flight tests on quadrotor and hexrotor validated the superiority of the controllers.

In recent work, we applied a L1 backstepping adaptive controller for hover attitude control of a flying wing VTOL MAV. Control effectiveness and wing aerodynamic moments varying with propeller slip stream are modeled in the control architecture. This procedure enables the adaptation law to concentrate on the identification and compensation of environmental disturbance. The controller outputs are desired moments, Dynamic Inversion(DI) is implemented to determine the movements of the actuators. Flight tests showed satisfactory tracking performance and prompt compensation of crosswind disturbance.As the controller includes nonlinear aerodynamic model and DI, it can be transplanted to other

VTOL MAV without retuning.

2　System Configuration

A flying wing tail-sitter MAV, named Novlit (Fig.1), was designed to perform hover, cruise and transitional flight. It has 60cm wing span and 450g takeoff weight. A pair of 10 inches coaxial contra rotating propellers is mounted to compensate each other's torque. The MH80 airfoil reflects a tradeoff between hover and cruise. This airfoil has relatively small pitch moment coefficient which makes hover trim easier, meanwhile, its moderate lift-drag performance satisfies cruise requirement. Elevon and rudder are immersed in the propeller slip stream to provide three axis control moments in hover.
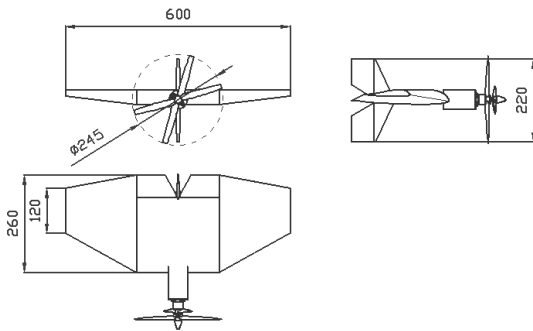

Fig. 1 Novlit tail-sitter MAV

　A customized autopilot (Fig.2) with dual STM32F405RG processors was used in recent work. One processor runs attitude estimation algorithm and sends state data package to the other processor with simplex communication, while the other processor is in charge of task management, control algorithm and data recorder. Such hardware architecture reduces the computational load of each processor, which enables the control algorithm runs at 200Hz and the data recorder runs at 100Hz.

We apply an explicit complementary filter(ECF) [7] to implement attitude estimation process. The ECF algorithm is more computational efficiency than widely used extended Kalman filter and unscented Kalman filter, while gaining similar accuracy. The coefficients of the ECF is

adopted for no GPS situation, which provides better dynamic response under small disturbance hover flight.

Fig. 2 Customized autopilot

3　Hover Attitude Controller

3.1　Dynamic Modelling

The attitude representation used throughout this paper is Euler angles. However, the conventional Euler angle is inapplicable for tail-sitter MAV in hover flight since the pitch angle (θ) is around $\frac{\pi}{2}$, then the roll (ϕ) and yaw (ψ) angles are not uniquely determined [5]. To fix this deficiency, we define a hover body coordinates. It is a right-handed body fixed coordinate system, whose origin is at the MAV center of gravity. Positive X_b axis points through the belly of the MAV, positive Y_b axis points out the right side, and positive Z_b axis points backward direction of the MAV fuselage, as shown in Fig.3. We call the corresponding Euler angle attitude representation the hover Euler angle.
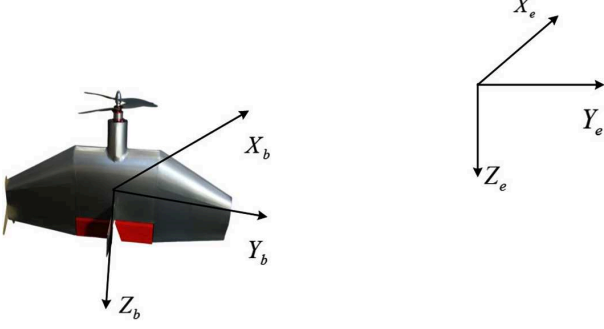
Fig. 3 Hover Body Coordinates

During hover flight, the pitch angle of the hover Euler angle is around 0 rather than $\frac{\pi}{2}$ as the conventional Euler angle is, which avoids the singularity. Another distinction is that the definition of the roll and yaw angles are interchanged. The roll angle now represents the angle between the horizontal surface and the connecting line of the right and left wingtips, while the yaw angle represents the rotation around the centerline of the MAV fuselage. The hover Euler angle will be used throughout this paper.

The attitude propagation equation is given as follows:

$$\dot{\Omega} = G\omega \qquad (1)$$

Where, $\dot{\Omega} = \begin{bmatrix} \dot{\phi} & \dot{\theta} & \dot{\psi} \end{bmatrix}^T$ are time derivatives of the hover Euler angle, $\omega = \begin{bmatrix} p & q & r \end{bmatrix}^T$ are body angular rates, G is the nonlinear propagation matrix defined as:

$$G = \begin{bmatrix} 1 & \sin\phi\tan\theta & \cos\phi\tan\theta \\ 0 & \cos\phi & -\sin\phi \\ 0 & \frac{\sin\phi}{\cos\theta} & \frac{\cos\phi}{\cos\theta} \end{bmatrix} \qquad (2)$$

The rotation dynamic equation can be represented as follows:

$$\dot{\omega} = H(\omega) + J^{-1}(\zeta\eta_c + \xi\eta_w + \upsilon) \qquad (3)$$

Where, $J \in R^{3\times3}$ is the matrix of the moment of inertia, $H(\omega) = -J^{-1}(\omega \times J\omega)$ represents the inertial coupling. $\eta_c = f_c(\alpha, V, T, \delta)$ and $\eta_w = f_w(\alpha, V, T, \delta)$ are aerodynamic moments generated by the control surfaces and the wing itself. The independent variables of these two nonlinear functions are angle of attack α, air speed of the vehicle V, propellers thrust T and

control surfaces deflection δ. ζ and ξ are the uncertainties of η_c and η_w, due to the imprecision of aerodynamic modeling and attitude estimation. υ is the uncertainty of the moment of inertia. These three coefficients reveal the source of the uncertainties. For controller derivation, we rearrange the latter part of Eq.3 as $J^{-1}(\eta_c + \eta_w + \sigma)$, where σ is defined as follows:

$$\sigma = (\zeta - I)\eta_c + (\xi - I)\eta_w + \upsilon$$

3.2 L1 Backstepping Attitude Controller

Regarding ω as a pseudo control, we apply backstepping control [6] as basal architecture of the L1 adaptive controller. ω_d represents the desired value of ω, and can be defined as follows:

$$\omega_d = G^{-1}(\dot{\Omega} + A_{m1}\tilde{\Omega}) \qquad (4)$$

Where $\tilde{\Omega} = \Omega - \Omega_d$, and A_{m1} is a Hurwitz matrix, which indicates exponential convergence of the Euler angles error. Then we define $\tilde{\omega} = \omega - \omega_d$, and derive the backstepping control architecture without uncertainties via the derivative of the following quadratic Lyapunov function:

$$V = \frac{1}{2}(\tilde{\Omega}^T\tilde{\Omega} + \tilde{\omega}^T\tilde{\omega})$$

whose derivative is as follows:

$$\begin{aligned} \dot{V} &= \dot{\tilde{\Omega}}^T\tilde{\Omega} + \dot{\tilde{\omega}}^T\tilde{\omega} \\ &= (G\omega - \dot{\Omega}_d)^T\tilde{\Omega} + (H(\omega) + J^{-1}\eta - \dot{\omega}_d)^T\tilde{\omega} \\ &= \tilde{\Omega}^T A_{m1}^T\tilde{\Omega} + (G^T\tilde{\Omega} + H(\omega) + J^{-1}\eta - \dot{\omega}_d)^T\tilde{\omega} \end{aligned}$$

Where $\eta = \eta_c + \eta_w$, thus we resolve the following control moments to keep the derivative negative:

$$\eta_c = -J(G^T\tilde{\Omega} + H(\omega) - J^{-1}\eta_w - \dot{\omega}_d - A_{m2}\tilde{\omega}) \qquad (5)$$

Where A_{m2} is a Hurwitz matrix that indicates exponential convergence of the angular rates error.

As the chief character of the L1 adaptive control theory is low pass filtered adaptive control signal, we may divide η_c into baseline part and adaptive part. The criterion for division is

distinguishable time delay, state noise and numerical stability due to differential. ω has minimum time delay and maximum measurement noise, Ω has medium time delay and noise due to the attitude estimation algorithm, $\dot{\omega}_d$ has wild fluctuation due to numerical differential. So we weigh the rapidity and the smoothness of the control signal, leave the baseline part eliminating ω error and the adaptive part compensating the identified uncertainties smoothly. The resultant L1 backstepping adaptive controller is composed of the following three parts: state predictor, adaptation law and control law.

3.2.1   State Predictor

The state predictor is defined as follows:

$$\dot{\hat{\omega}} = H(\omega) + J^{-1}(\eta + \hat{\sigma}) + A_{sp}(\hat{\omega} - \omega) \quad (6)$$

Where $\hat{\sigma}$ is the estimate of the uncertainties which will be defined in the following section. $\hat{\omega}$ is the angular rate estimate, A_{sp} is a Hurwitz matrix used to confirm the estimate dependency upon the angular rate measurements. Setting a large A_{sp} makes $\hat{\omega}$ prefer to track the angular rate measurements tightly, otherwise, the fore part of Eq.6 becomes more crucial, what makes $\hat{\omega}$ prefer to identify the uncertainties facilely.

3.2.2   Adaptation Law

we define the adaptation law as follows:

$$\hat{\sigma}(t) = JA_{sp}(I - exp(A_{sp}T_s))^{-1}exp(A_{sp}T_s)e(iT_s)$$
$$\forall t \in [iT_s, (i+1)T_s] \ \ i = 1, 2, 3, \ldots \quad (7)$$

Where T_s is the sampling time of the control algorithm, $e = \hat{\omega} - \omega$ indicates the prediction error. All the other part of Eq.7 resolves the adaptation gain corresponding to T_s and A_{sp}, while the differences in the moment of inertia are normalized accordingly.

3.2.3   Control Law

Finally, the control signal is generated as follows:

$$\eta_c = \eta_b + \eta_a \quad (8)$$
$$\eta_b = -J(H(\omega) - J^{-1}\eta_w - A_{m2}\tilde{\omega}) \quad (9)$$

$$\eta_a(s) = KD(s)\tau(s) \quad (10)$$
$$\tau = \eta_a + \hat{\sigma} - J\dot{\omega}_d$$

where η_b is the baseline part, and η_a is the adaptive part. K is a positive gain, $D(s)$ is a strictly proper transfer function, they yield a BIBO stable strictly proper transfer function $C(s)$, with the unity DC gain:

$$C(s) = \zeta KD(s)(I + \zeta KD(s))^{-1} \quad (11)$$

Since the estimate of uncertainties $\hat{\sigma}$ is low pass filtered by $C(s)$, the compensation of $\hat{\sigma}$ will be smoother, so is the response to $\dot{\omega}_d$. Tuning K and $D(s)$ adjusts the bandwidth of the adaptive part of the control signal. This ensures the controller only responding to the uncertainties within the natural frequency of the MAV, which suggests that the fast estimate of the uncertainties is acceptable without hurting the system robustness. This character indicates better disturbance identification and compensation.

4   Flight Validation

4.1   Implementation of the Controller

Since the proposed hover attitude controller is capable of the compensation of uncertainties, including model error, the fidelity of vortex lattice method (VLM) meets the demand of aerodynamic modeling. We apply the VLM method to obtain aerodynamic coefficients as a timesaver. During hover flight, almost all aerodynamic moments are generated by the slip stream of the propellers, a corresponding estimation method proposed by Kubo and Suzuki [8] is applied.
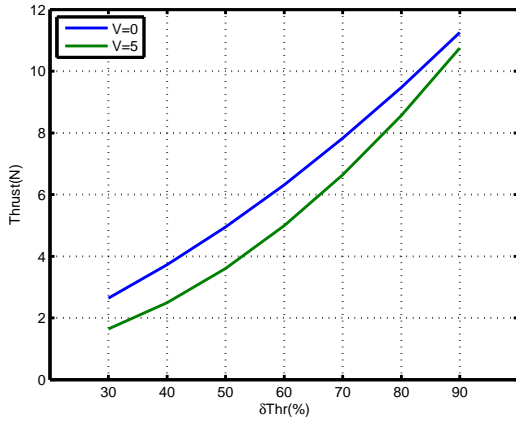
Fig. 4 Propeller Wind-Tunnel Experiment

Fig. 5 Thrust vs δ_T

Firstly, the propeller thrust and rotate speed which vary with the throttle setting (Fig.5) are measured via wind-tunnel experiment (Fig.4). then the propeller-induced velocity and the diameter of the stream tube are calculated using one dimensional momentum theory. the wing is divided into immersed and non-immersed in the propeller slip stream portions, the aerodynamic moments of each portion are calculated separately. The immersed portion employs the propeller-induced velocity at the quarter chord as the air velocity, while the air velocity of the non-immersed portion can be ignored in hover flight. According to the results of the above procedure, the controller resolves η_w from the throttle setting using linear interpolation of the following quadric fitting function.

$$\eta_w = \Delta(\kappa_1 \delta_T^2 + \kappa_2 \delta_T + \kappa_3)(C_0 + C_\omega \omega) \quad (12)$$

Where $\delta_T \in [0.5, 0.7]$ is the hover throttle setting, C_0 is the moment coefficient at zero angle of attack of the three axis, correspondingly, C_ω is the moment coefficients due to angular rates. Δ, κ_1, κ_2, κ_3 are the coefficients of the fitting function. Since the controller output is control moment η_c, the actual control surfaces deflection δ_c should be determined from η_c. This is an inverse process of calculating control moments, so it is called output Dynamic Inversion(DI):

$$\delta_c = \frac{\eta_c}{\Delta(\kappa_1 \delta_T^2 + \kappa_2 \delta_T + \kappa_3)C_\delta} \quad (13)$$

Where C_δ is the moment coefficients due to control surfaces deflection, and the coefficients of the fitting function are same as Eq.12. Since the recent work focuses on the hover attitude control, the outer-loop Euler angle commands are given by the operator via R/C system, and the throttle setting command is directly from R/C system. To ensure the continuity of ω_d and $\dot{\omega}_d$, the inputs from the R/C system need to be second order low-pass filtered. The damping ratio and natural frequency of the filter depend on the operator's control habit. In this paper, we select 0.85 damping ratio and $45 rad/s$ natural frequency, thus the filter is able to smoothing 1Hz~3Hz Euler angle commands properly.

4.2 Flight Tests Results and Analysis

Fig. 6 Novlit MAV in Hover Flight

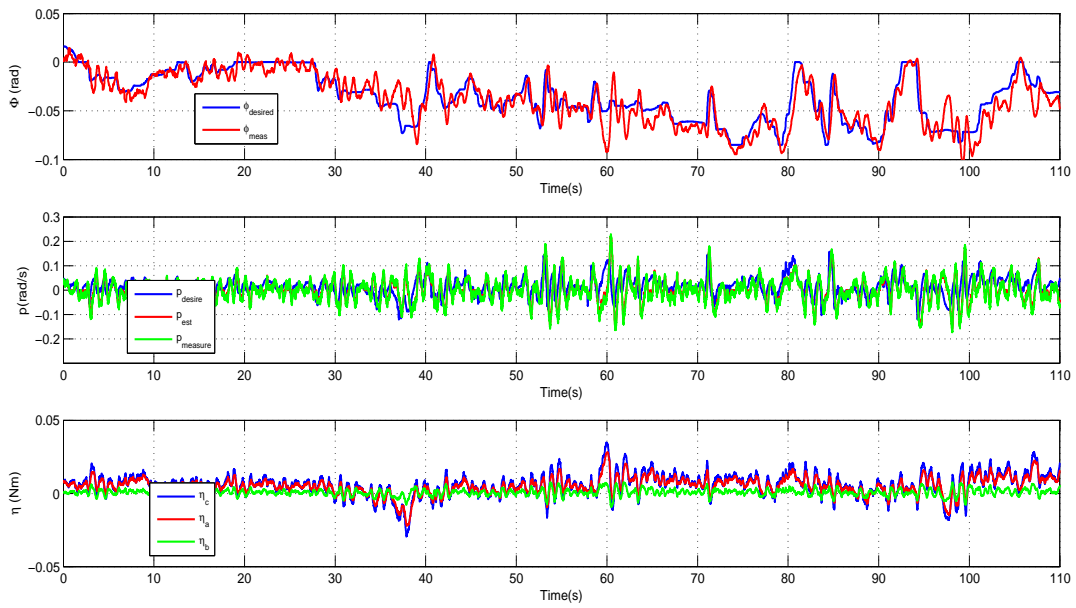Flight tests were carried out both indoor and outdoor. The indoor hover flight showed the

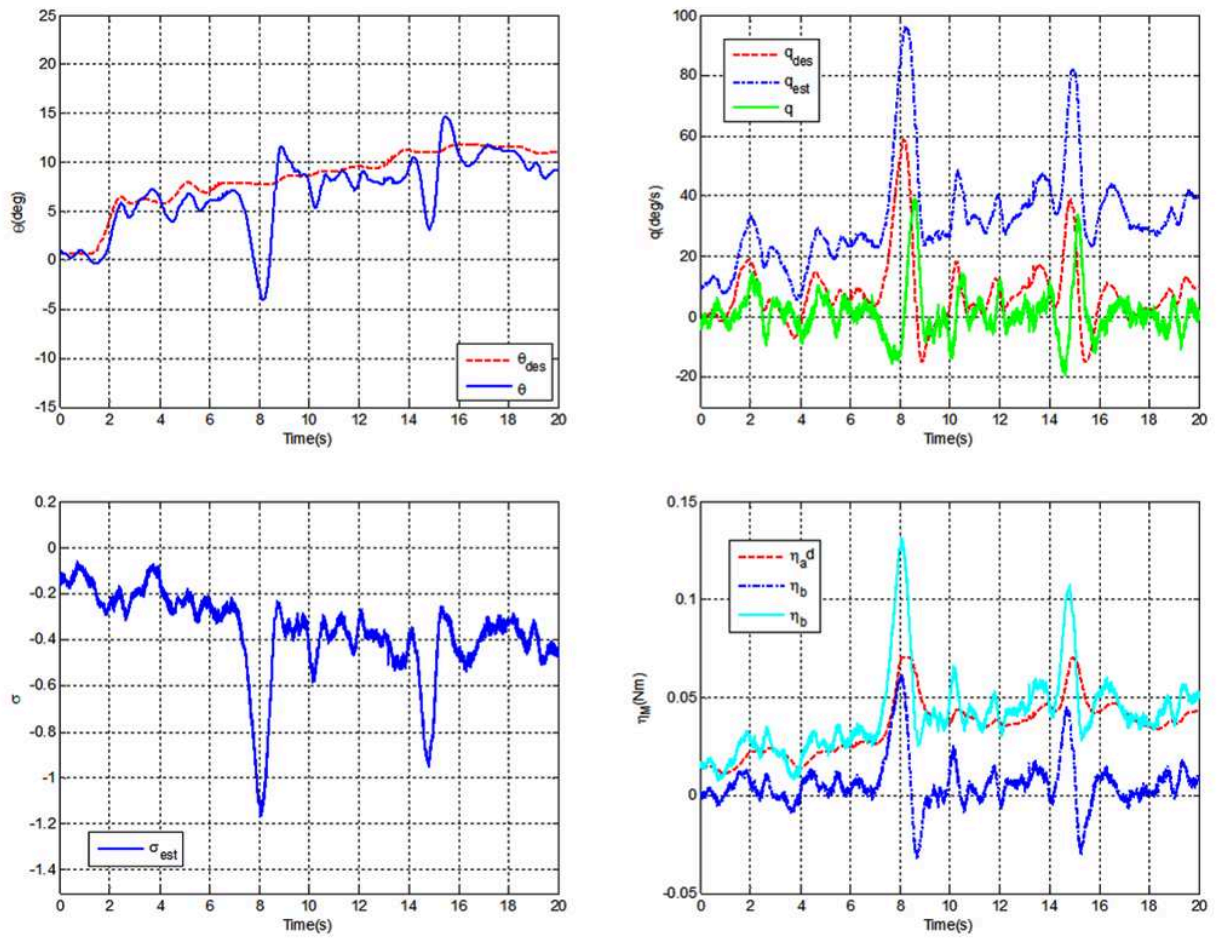**Fig. 7** Indoor Flight Test Results

Fig. 8 Outdoor Flight Test Results

tracking performance of the proposed L1 backstepping controller while the outdoor hover flight revealed the compensation of crosswind disturbance.(Fig.6)

Fig.7 shows an indoor hover flight lasting about 2 minutes. The roll angle ϕ follows the desired roll angle ϕ_{desire} within one degree deviation, since the roll angular rate p achieves the desired roll angular rate p_{desire} with a coincident time delay around 40ms. The roll angular rate estimate $\hat{p}$ tightly follows the roll angular rate p, which indicates that there is no appreciable model error or environmental disturbance. Consequently, η_a acts as an augmentation part which improves the tracking performance of the MAV.

Fig.8 show outdoor hover flight test results. The controller tracks the desired pitch angle θ_{desire} and the corresponding pitch angular rate q_{desire}. It should be noted that the prominent perturbations around 8s and 15s are caused by crosswind, they are identified as the estimate of the uncertainty $\hat{\sigma}$ and quickly compensated by filtered adaptive control signal η_a , the pitch angle is stabilized with acceptable deviation.

5   Summary and Future Work

This work presented a L1 backstepping adaptive control architecture for hover attitude control of a tail-sitter VTOL MAV, the indoor and outdoor flight tests validated its tracking performance and fast adaptation. Nonlinear aerodynamic model is contained to ensure the adaptation law to concentrate on the environmental disturbance. Since the L1 control theory ensures fast adaptation and robustness of the close-loop system, the less time-consuming aerodynamic model method VLM and one dimensional momentum theory meet the accuracy requirement of the controller. The output of the proposed controller is control moment, the output dynamic inversion is applied to resolve the control surface deflection. These characters, together with the inherent advantages of L1 adaptive control scheme, make the proposed architecture a consistent solution for hover attitude control of various VTOL MAVs.

In recent work, the Euler angle commands are generated by the operator. We should integrate the outer-loop position controller into the present L1 backstepping attitude controller, achieving spot hover will be the next aim.

L1 adaptive control theory deals with linear state space control problems. Since the presented L1 adaptive controller with backstepping architecture transforms the cascade nonlinear dynamics system into a linear-liked form, the controller can be viewed as a particular realization form of L1 adaptive control theory. The corresponding systematic design procedure similar to the other L1 controllers is still absent. The theoretical derivation of the L1 norm condition and the performance bounds of the presented controller will remain a meaningful open problem.

References

[1] Jung Y,Shim D.Development and Application of Controller for Transition Flight of Tail-Sitter UAV.*Journal of Intelligence Robot System*,Vol. 65,No. 4,pp 137-152,2012.

[2] Takaaki Matsumoto,Koichi Kita et al.A Hovering Control Stratagy for a Tail-Sitter VTOL UAV that Increases Stability Against Large Disturbance.*2010 IEEE International Conference on Robotics and Automation*,Anchorage,Alaska,USA,Vol. 10,978-1-4244-5040-4,pp 54-59,2010.

[3] Naira Hovakimyan,Chengyu Cao.*L1 Adaptive Control Theory—Guaranteed Robustness with Fast Adaptation*Society for Industrial and Applied Mathematics,2010.

[4] Srinath Mallikarjunan,Bill Nesbitt et al. L1 Adaptive Controller for Attitude Control of Multirotors.*AIAA Guidance,Navigation,and Control Conference*,Minneapolis,Minnesota,USA,AIAA 2012-4831,2012.

[5] W Phillips,C Hailey.Review of Attitude Representations Used for Aircraft Kinematics.*Journal of Aircraft*,Vol. 38,No. 4,pp 718-737,2001.

[6] Kristic M,Kanellakopoulos I.*Nonlinear and Adaptive Control Design*John Wiley & Sons,1995.

[7] Pierre-Richard Bilodeay,Eric Poulin et al.

Attitude Estimation and Control of a Hovering Mini Aerial Vehicle.*AIAA Guidance,Navigation,and Control Conference*, Toronto, Ontario, Canada, AIAA 2010-8417, 2010.

[8] Daisuke Kubo,Shinji Suzuki.Tail-Sitter Vertical Takeoff and Landing Unmanned Aerial Vehicle:Transitional Flight Analysis.*Journal of Aircraft* ,Vol. 45,No. 1,pp 292-297,2008.

Contact Author Email Address

mailto:wangjin_nwpu@163.com

Copyright Statement